Climate change and aircraft turbulence

Paul D. Williams, University of Reading

THE ROYAL SOCIETY

National Centre for Atmospheric Science
NATURAL ENVIRONMENT RESEARCH COUNCIL

University of Reading

Can we use a radiosonde to directly measure turbulence?

- Turbulence strength can be estimated from HVRRD vertical profiles using the Thorpe (1977) method (e.g. Geller et al. 2021, Ko & Chun 2022)
- But can we measure it more directly?
- When a balloon encounters turbulence it will cause the balloon to move about its average trajectory
- Consider the balloon and radiosonde payload to be a pendulum with a moving pivot
- Rapid changes in the balloon's trajectory cause the payload to swing beneath the balloon
- More intense turbulence causes larger swings in the payload beneath – can we measure these swings?

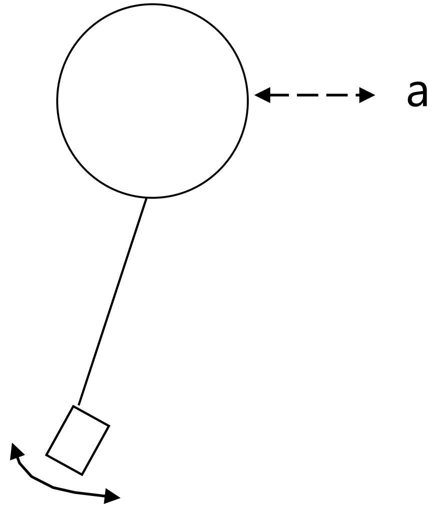

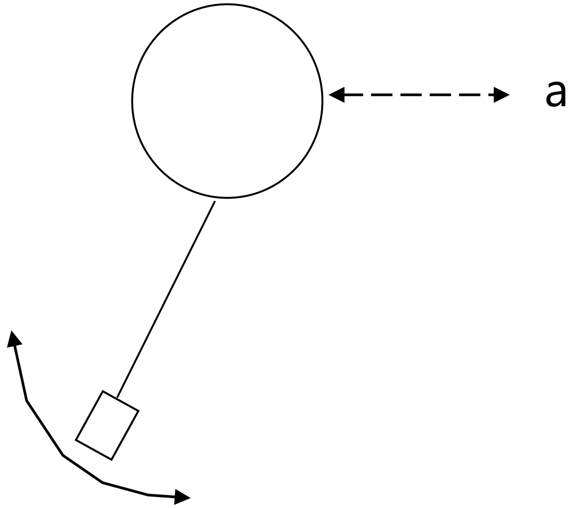

Nintendo Wii uses motion gesture technology for game interaction.

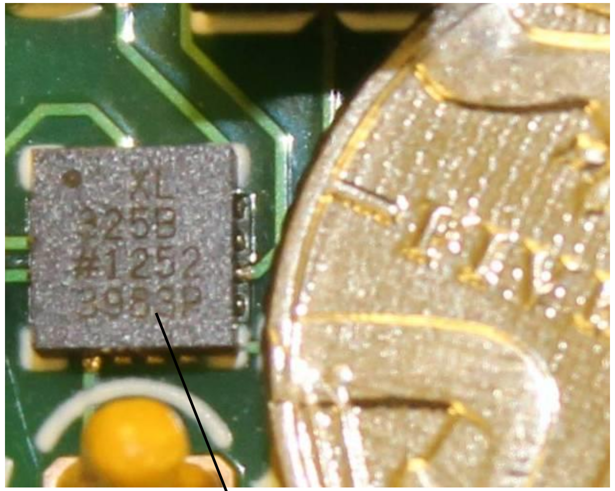

Achieved using accelerometer to measure sonde's motion.

Use ADXL 325, a three-axis +/- 5g minimal range accelerometer.

Add additional electronics to power accelerometer and modulate accelerometer outputs.

Connect to data acquisition system and attach box to sensing package.

Capacitive Accelerometer Mechanism

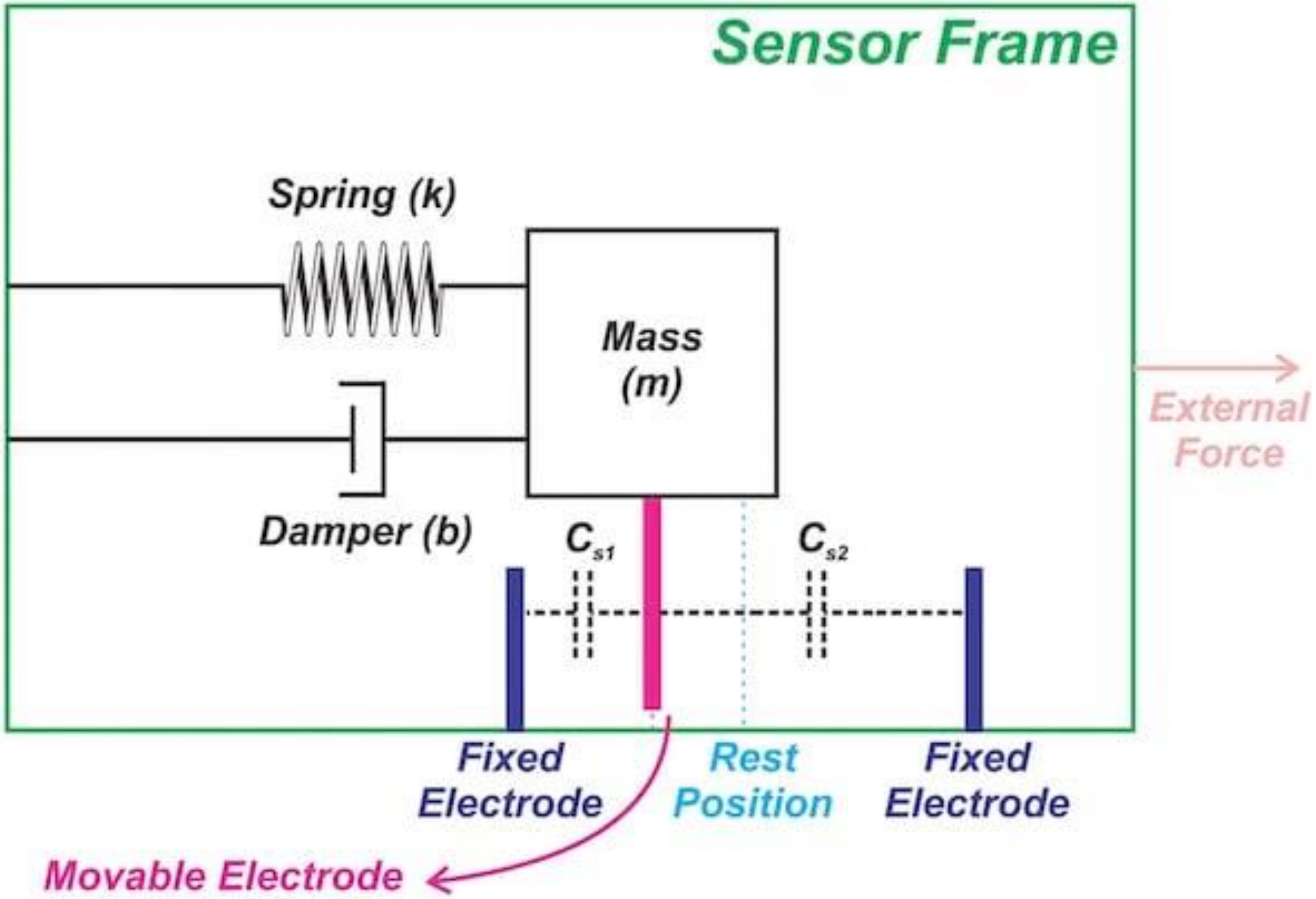

Additional sensor measurement system

We have developed a system which adds extra data channels for new sensors.

The system, named Programmable ANalogue and Digital Radiosonde Accessory (PANDORA), is placed in a small box and attached to the radiosonde.

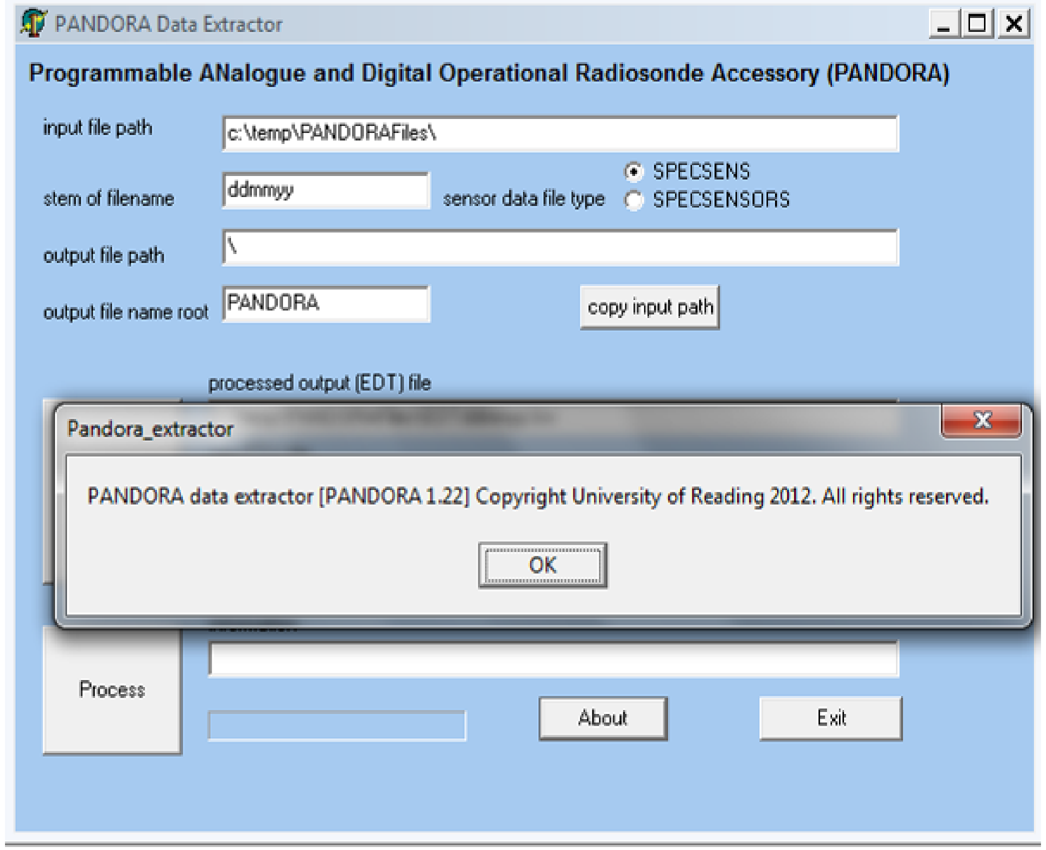

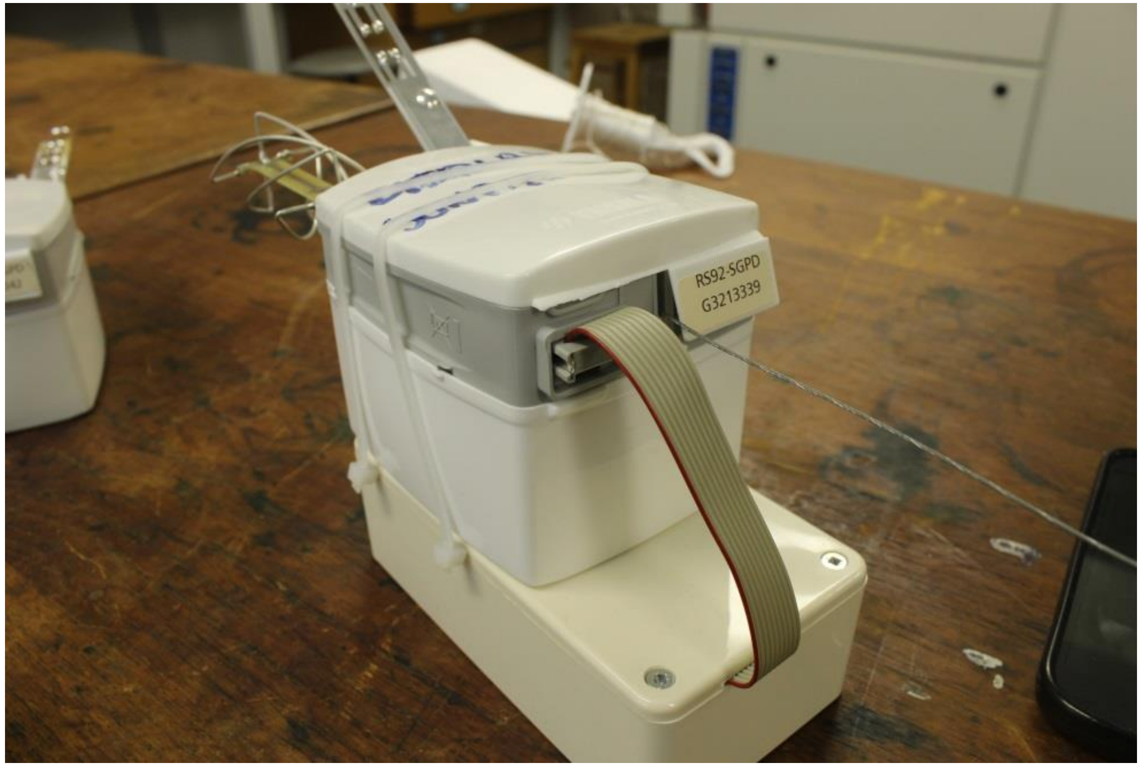

PANDORA is connected to the sonde through the Ozone port to relay data over radio link

No additional hardware needed.

PANDORA extractor retrieves the data and synchronises it with standard meteorological quantities

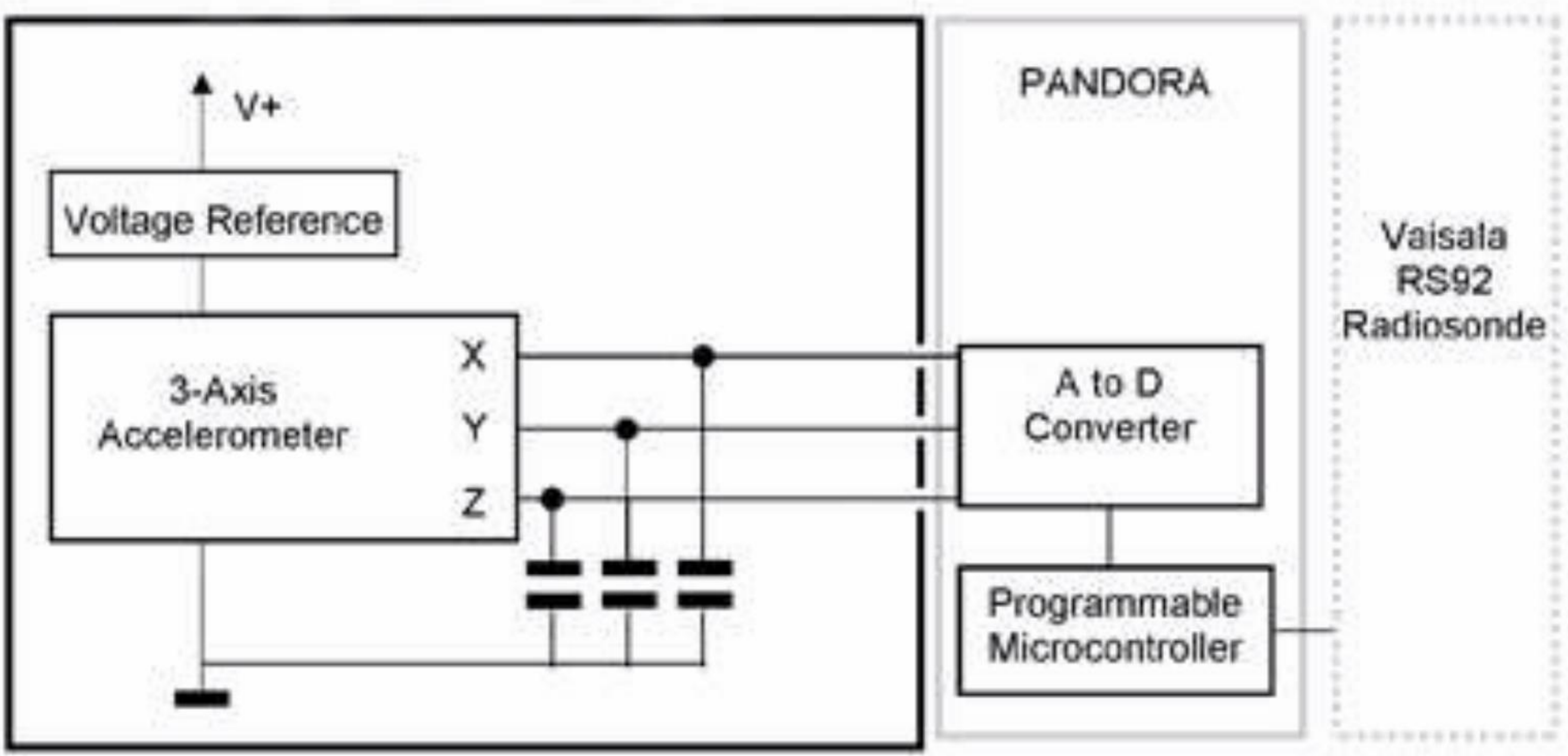

V+
Voltage Reference
3-Axis
Accelerometer
X
Y
Z
PANDORA
A to D
Converter
Programmable
Microcontroller
Vaisala
RS92
Radiosonde

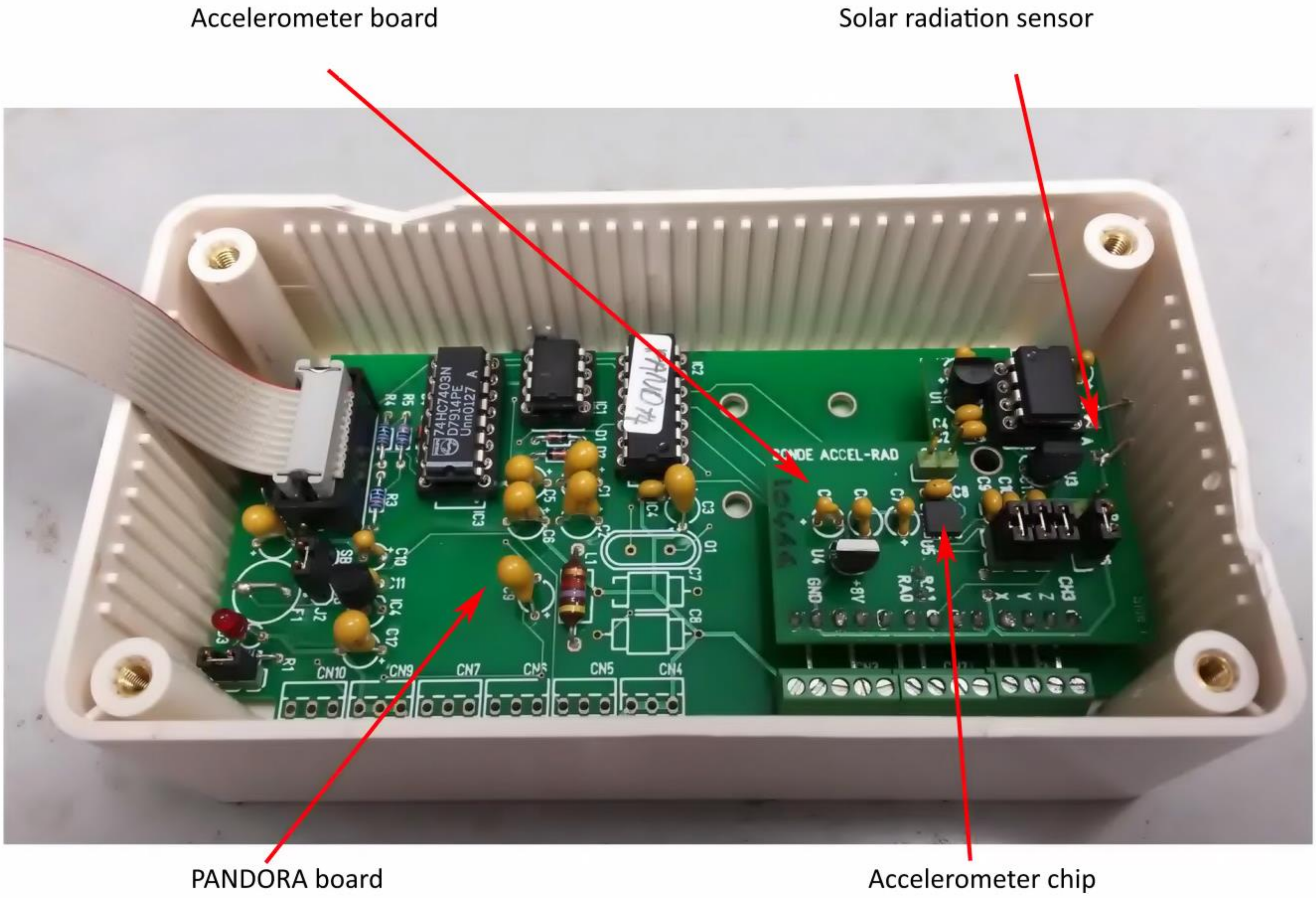
Accelerometer board
Solar radiation sensor
PANDORA board
Accelerometer chip

Calibration between voltage and acceleration

	ADXL355	ADXL325
Minimal range	$\pm$ 3g	$\pm$ 5g
Z-axis sensitivity	245 mV g^{-1}	-190$\pm$2 mV g^{-1}
Z-axis offset	-1300 mV	-1674$\pm$2 mV
Y-axis sensitivity	240 mV g^{-1}	193$\pm$2 mV g^{-1}
Y-axis offset	-1300 mV	-1643$\pm$2 mV
X-axis sensitivity	260 mV g^{-1}	185$\pm$2 mV g^{-1}
X-axis offset	-1300mv	-1683$\pm$1 mV

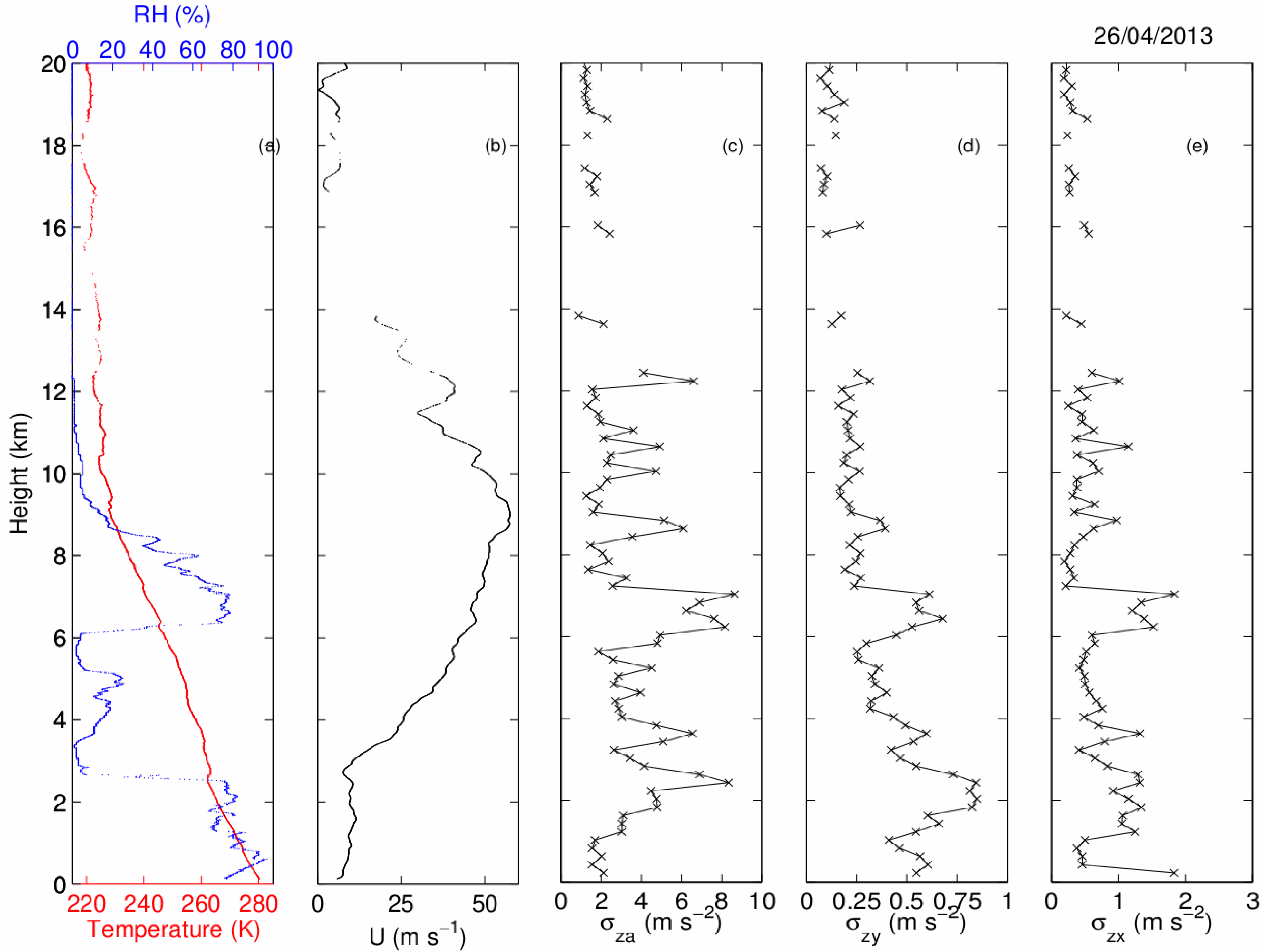

26/04/2013
RH (%)
0 20 40 60 80 100
Height (km)
(a)
(b)
(c)
(d)
(e)
220 240 260 280
Temperature (K)
0 25 50
U (m s^{-1})
0 2 4 6 8 10
σ_{za} (m s^{-2})
0 0.25 0.5 0.75 1
σ_{zy} (m s^{-2})
0 1 2 3
σ_{zx} (m s^{-2})

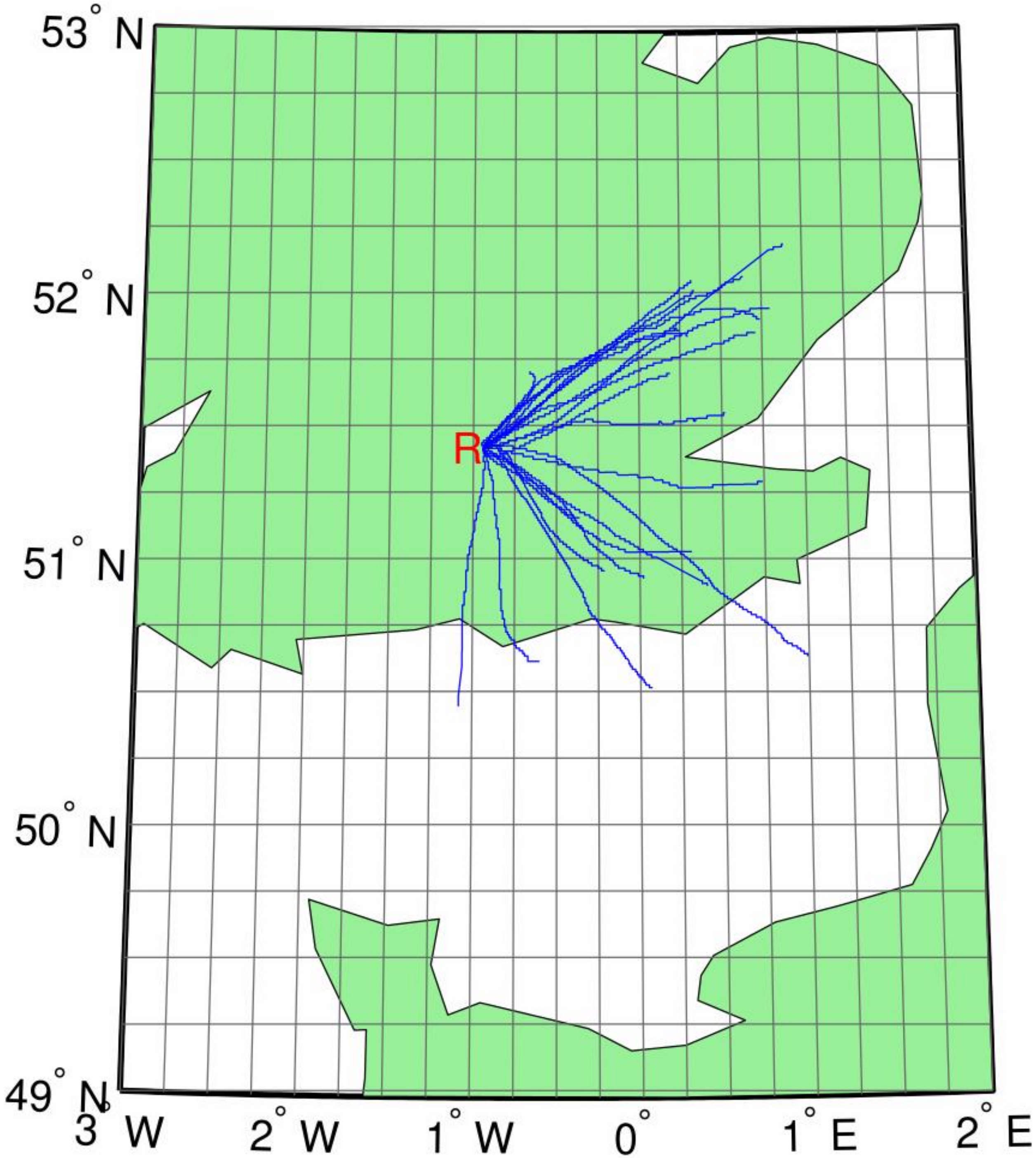

53° N
52° N
51° N
50° N
49° N
3° W
2° W
1° W
0°
1° E
2° E
R

Strategy and summary of flights

Strategy:

- To launch accelerometer balloons into different weather conditions to gather as much information on different types of turbulence.
- To compare turbulence observations with CAT diagnostics from NWP data.

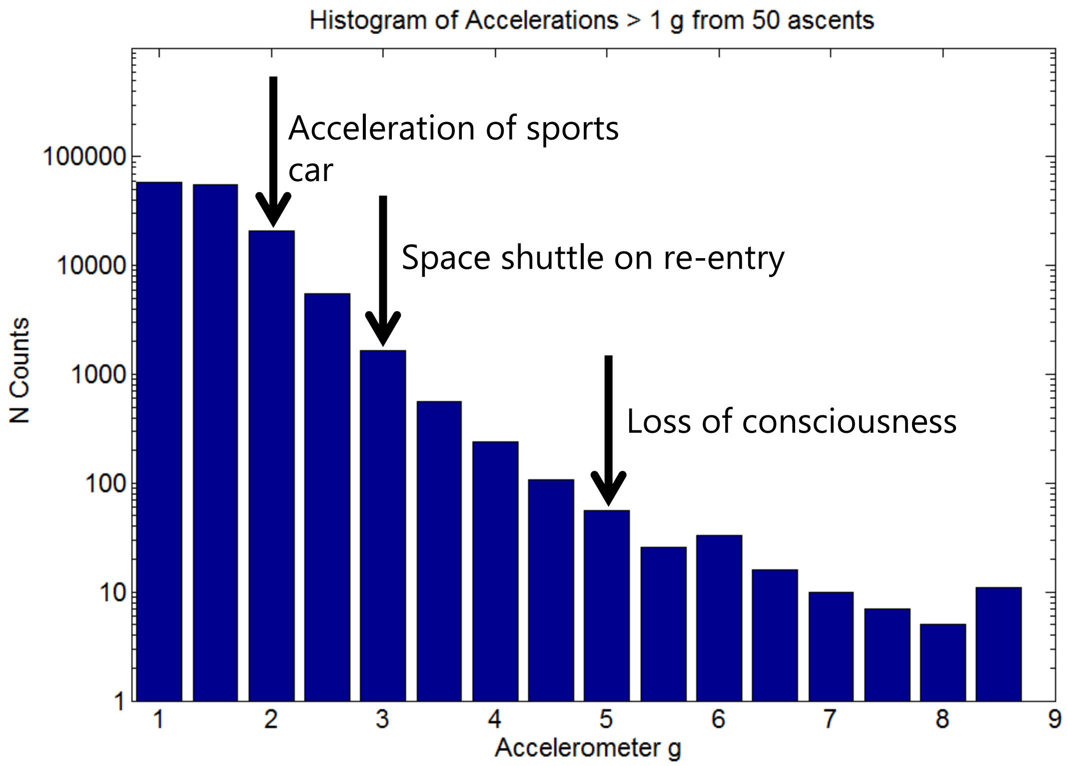

Over 50 flights have been made from Reading and other locations across the UK and Europe.

Histogram summarises the accelerometer results from these ascents.

Comparisons have been made with:

1. Lidar in Reading, UK
2. Cloud radar in Hyytiala Finland
3. Wind profiler at Aberystwyth, UK

Diagnostic	Symbol	Units	Equation no.
-ve Richardson number	$-Ri$		B.4
Colson Panofsky index	CP	knots^2	B.5
Knox 1997 index	$KX1$	s^{-2}	B.26
Relative vorticity squared	ξ^2	s^{-2}	B.10
North Carolina State University index 1	$NCSU1$	s^{-3}	B.23
Brown index	Φ	s $^{-1}$	B.11
Brown eddy dissipation rate	ϵ_{Brown}	m^{2}s^{-3}	B.13
Ellrod's turbulence index 1	$ET1$	s^{-2}	B.15
Ellrod's turbulence index 2	$ET2$	s^{-2}	B.16
U $\times$ Deformation	$UDEF$	m s^{-2}	B.21
Thermal gradient $\times$ Deformation	T_zDEF	K m^{-1}s^{-1}	B.22
Frontogenesis function	F	m^2 s^{-3} K^{-2}	B.8
Potential vorticity	$\|PV\|$	m^{2}s^{-1}K kg^{-1}	B.17
Negative absolute vorticity advection	$NAVA$	s^{-2}	B.24
Vertical wind shear	U_z	s^{-1}	B.3
Horizontal temperature gradient	$\|\nabla_H T\|$	K m^{-1}	B.18
Clark's CAT algorithm	$CCAT$	s^{-3}	B.27
Dutton empirical index	DUT	s^{-2}	B.28
Relative vorticity advection	$\|RVA\|$	s^{-2}	B.25
Wind speed	U	m s^{-1}	B.19
Wind speed $\times$ directional shear	$U\phi_z$	rad s^{-1}	B.20
Horizontal divergence	$\|\nabla_H\|$	s^{-1}	B.14
Flow Deformation	DEF	s^{-1}	B.9

Case study comparison with CAT diagnostics

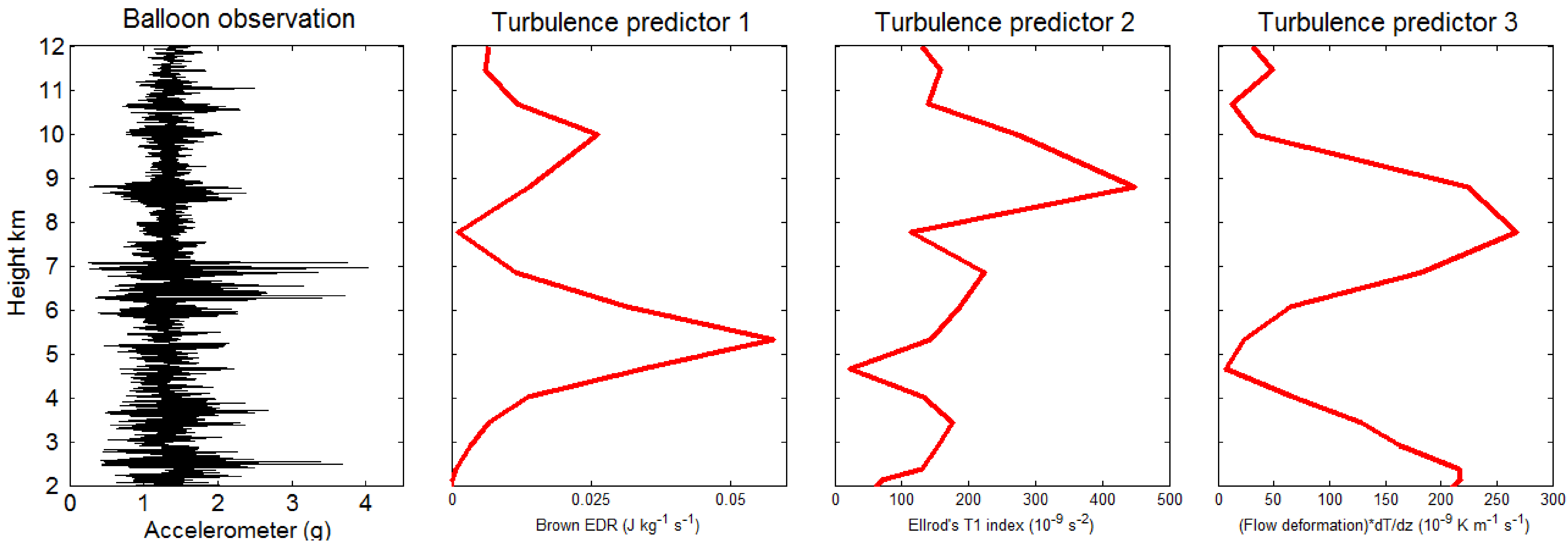

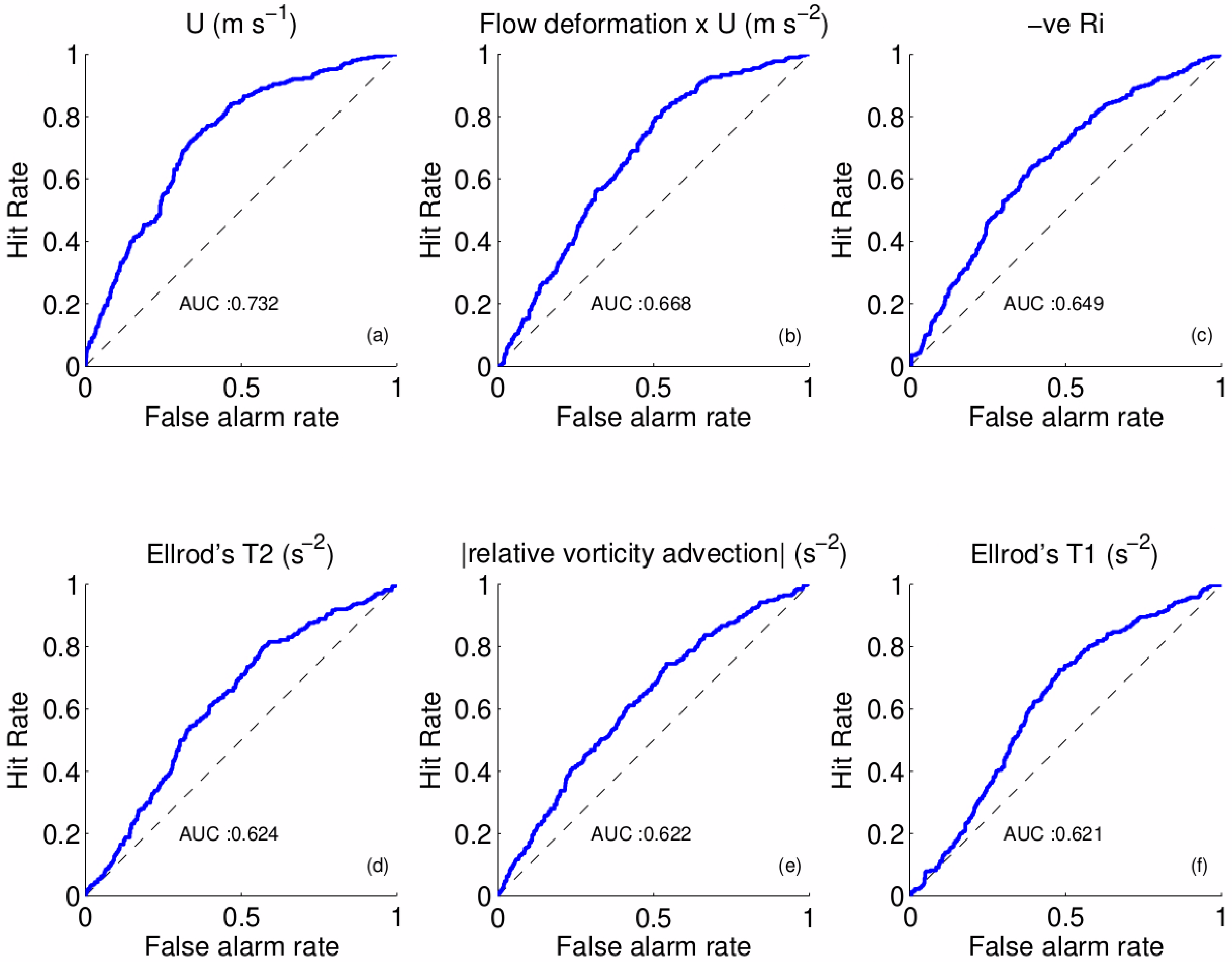

U (m s⁻¹)
AUC :0.732
(a)
Flow deformation x U (m s⁻²)
AUC :0.668
(b)
−ve Ri
AUC :0.649
(c)
Ellrod's T2 (s⁻²)
AUC :0.624
(d)
|relative vorticity advection| (s⁻²)
AUC :0.622
(e)
Ellrod's T1 (s⁻²)
AUC :0.621
(f)
Hit Rate
False alarm rate
0
0.2
0.4
0.6
0.8
1
0.5

Diagnostic	Units	Exp. 1 AUC	Exp. 2 AUC	Optimal threshold
U	m s^{-1}	0.675±0.022	0.732±0.008	>35.2573
$UDEF$	m s^{-2}	0.653±0.021	0.668±0.016	> 0.0014
$-Ri$		0.592±0.016	0.649±0.021	>-5.245
$ET2$	s^{-2}	0.628±0.024	0.624±0.013	> 3.726e-07
$\|RVA\|$	s^{-2}	0.602±0.012	0.622±0.012	>9.8827e-09
$ET1$	s^{-2}	0.619±0.014	0.621±0.008	>3.012e-07
U_z	s^{-1}	0.583±0.019	0.613±0.006	> 0.0070
ϵ_{brown}	m^2s^{-3}	0.595±0.016	0.613±0.008	>1.5126e-10
DUT	s^{-2}	0.582±0.015	0.598±0.013	>22.0602
T_zDEF	K m^{-1} s^{-1}	0.585±0.028	0.580±0.008	>2.323e-07
$U\phi_z$	rad (s^{-1})	0.553±0.012	0.570±0.005	>1.549
$KX1$	s^{-2}	0.542±0.018	0.560±0.012	>1.6289e-08
$\|\nabla_H\|$	s^{-1}	0.545±0.026	0.546±0.018	>2.5539e-05
$CCAT$	s^{-3}	0.565±0.020	0.539±0.009	>7.0333e-09
DEF	s^{-1}	0.582±0.019	0.537±0.008	>5.2487e-05
CP	$knot^2$	0.510±0.020	0.531±0.007	>-162.2705
ξ^2	s^{-2}	0.572±0.029	0.526±0.013	>9.7652e-10
$\|\nabla_H T\|$	K m^{-1}	0.536±0.021	0.521±0.008	>1.3887e-05
$NAVA$	s^{-2}	0.517±0.017	0.513±0.006	> 4.0524e-09
Φ	s^{-1}	0.553±0.024	0.494±0.007	<8.2372e-05
$\|PV\|$	m^2s^{-1}K kg^{-1}	0.507±0.025	0.483±0.014	< 1.2152e-06
$NCSUI1$	s^{-3}	0.461±0.012	0.458±0.007	<7.336e-18
F	m^2 s^{-3} K^{-2}	0.446±0.018	0.431±0.015	<-1.8417e-06

Impacts of climate change on the jet stream

Temperature changes driven by CO_2 in IPCC climate simulations

Stronger north–south temperature gradient at flight cruising altitudes

$$\frac{\partial u}{\partial z} \propto -\frac{\partial T}{\partial y}$$

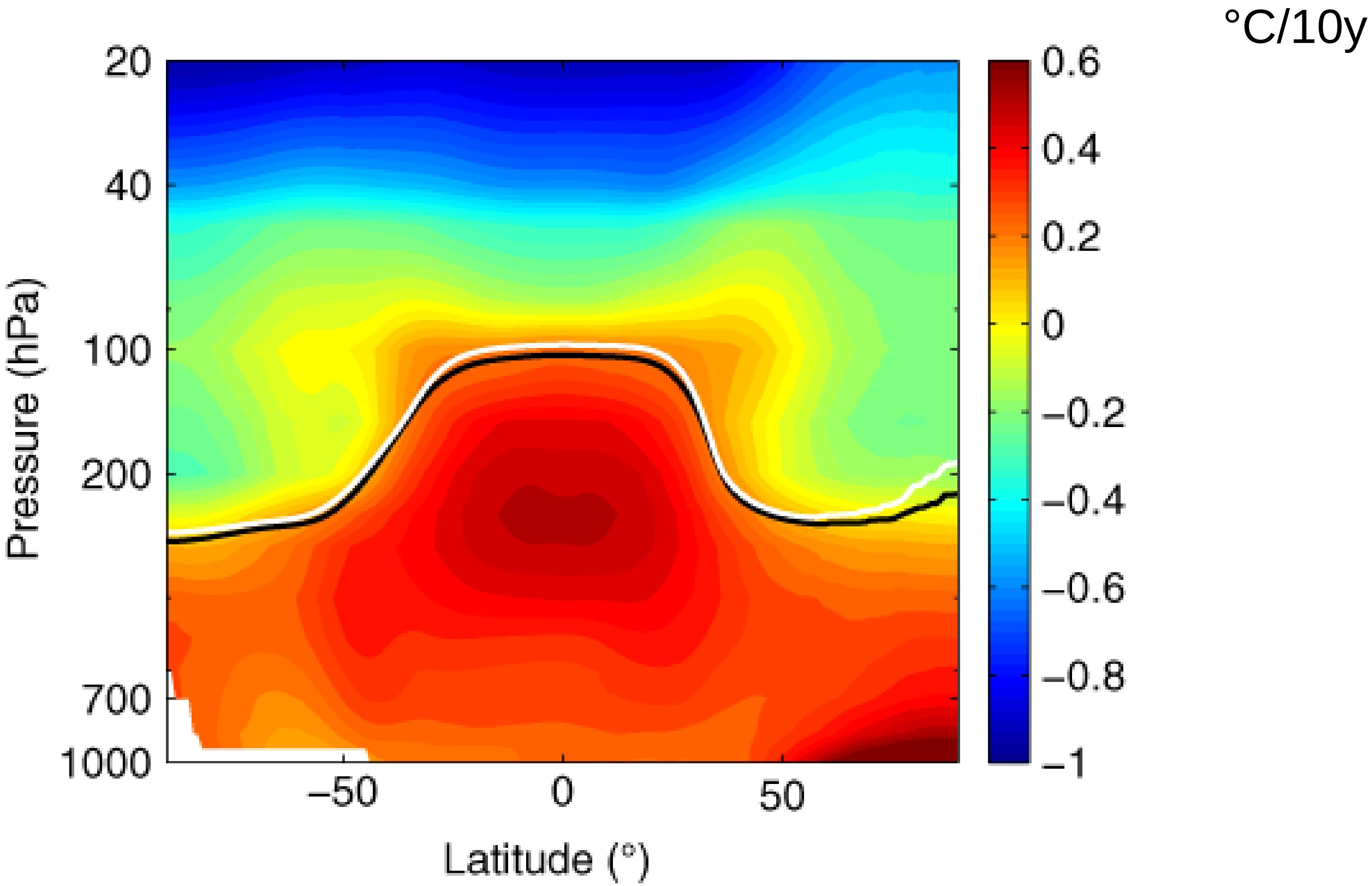

Vallis et al. (2015)

Impacts of climate change on the jet stream

Temperature changes 1960–2012 measured by radiosondes

Stronger north–south temperature gradient at flight cruising altitudes

$$\frac{\partial u}{\partial z} \propto -\frac{\partial T}{\partial y}$$

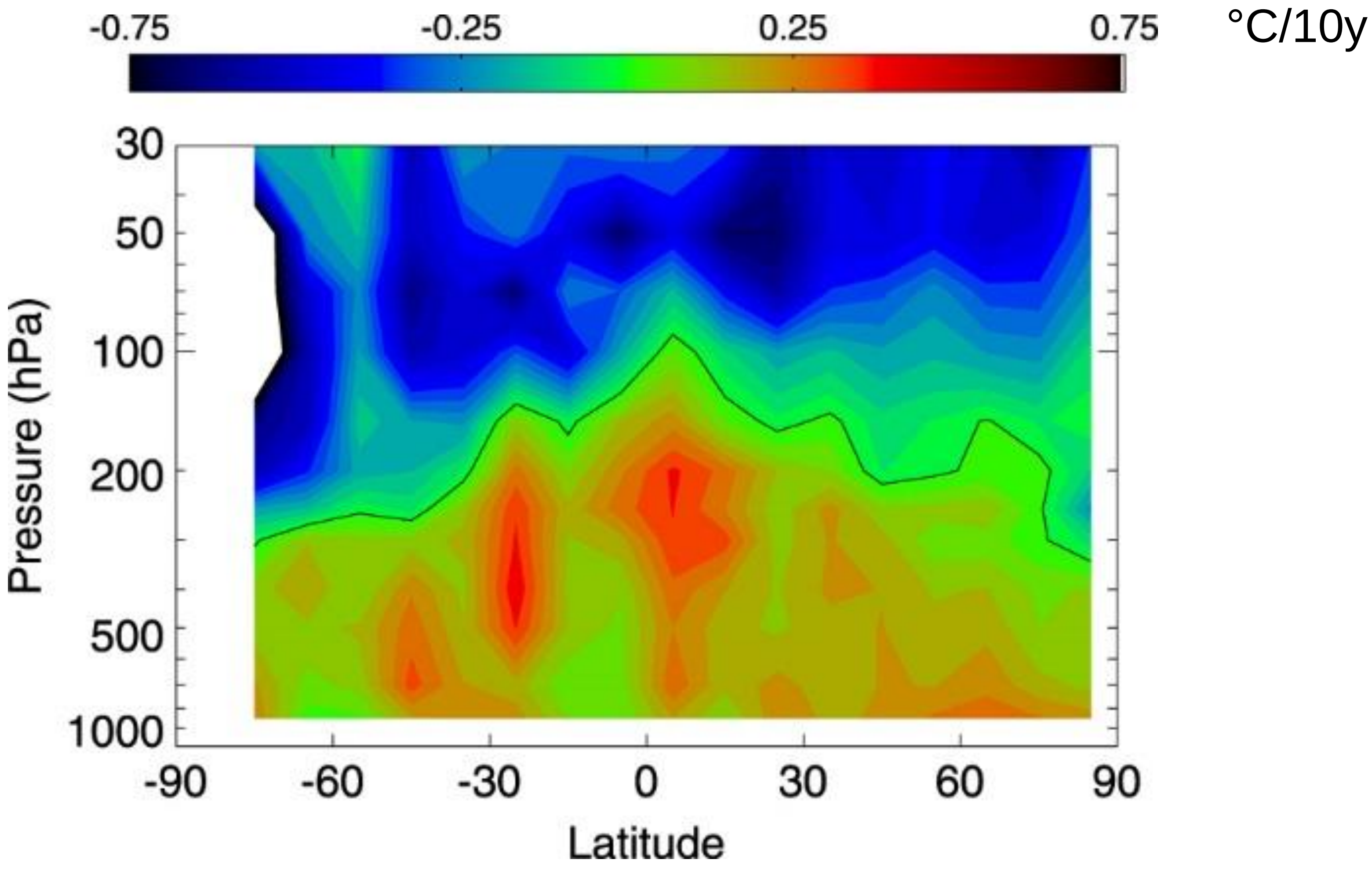

Sherwood & Nishant (2015)

Impacts of climate change on the jet stream

Temperature changes 1979–2017 at 250 hPa in reanalysis data

Stronger north–south temperature gradient at flight cruising altitudes

$$\frac{\partial u}{\partial z} \propto -\frac{\partial T}{\partial y}$$

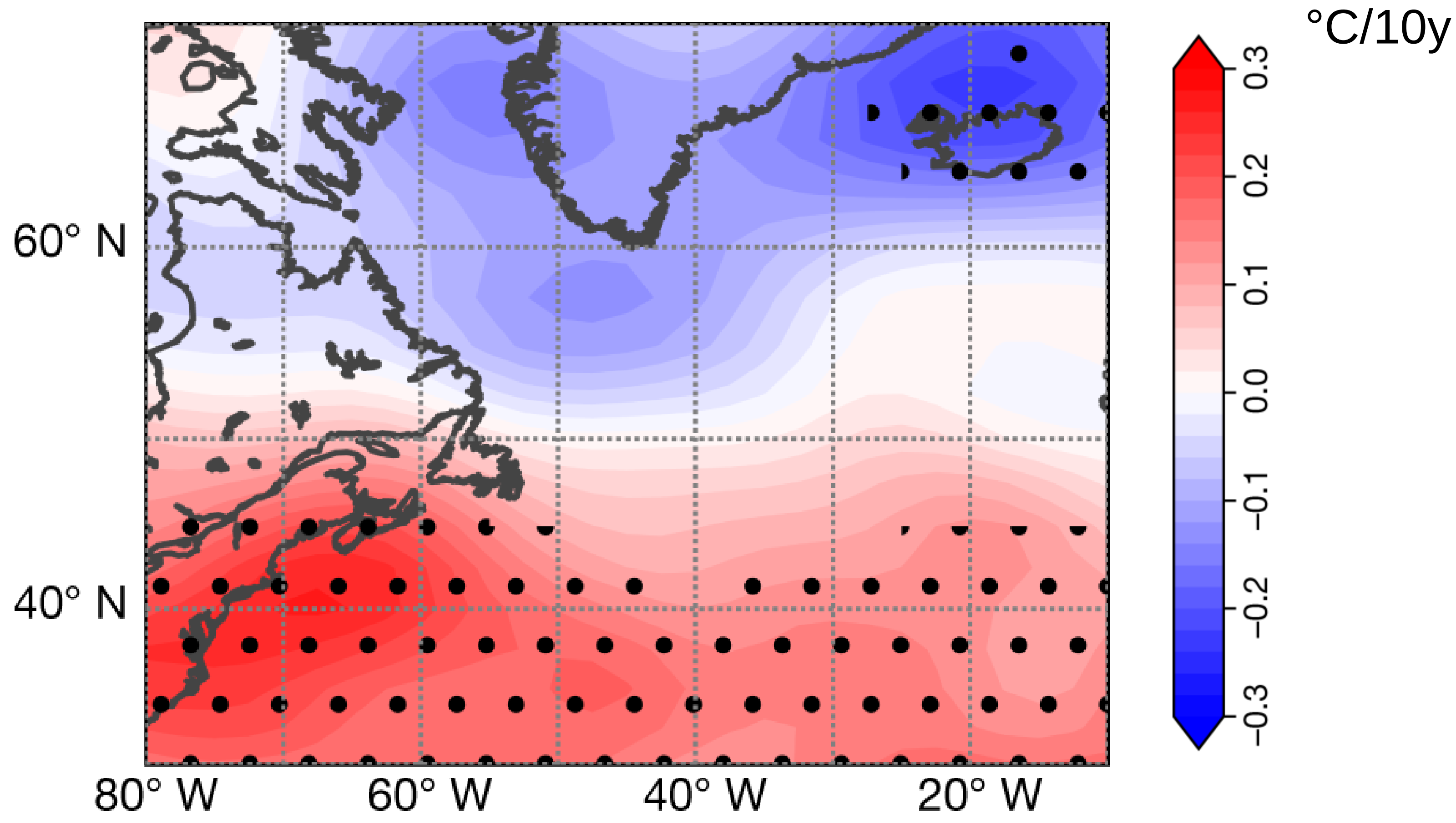

Lee, Williams, and Frame (2019)

Impacts of climate change on the jet stream

Zonal wind changes driven by CO_2 in IPCC climate simulations

Stronger eastward winds & windshears at flight cruising altitudes

$$\frac{\partial u}{\partial z} \propto -\frac{\partial T}{\partial y}$$

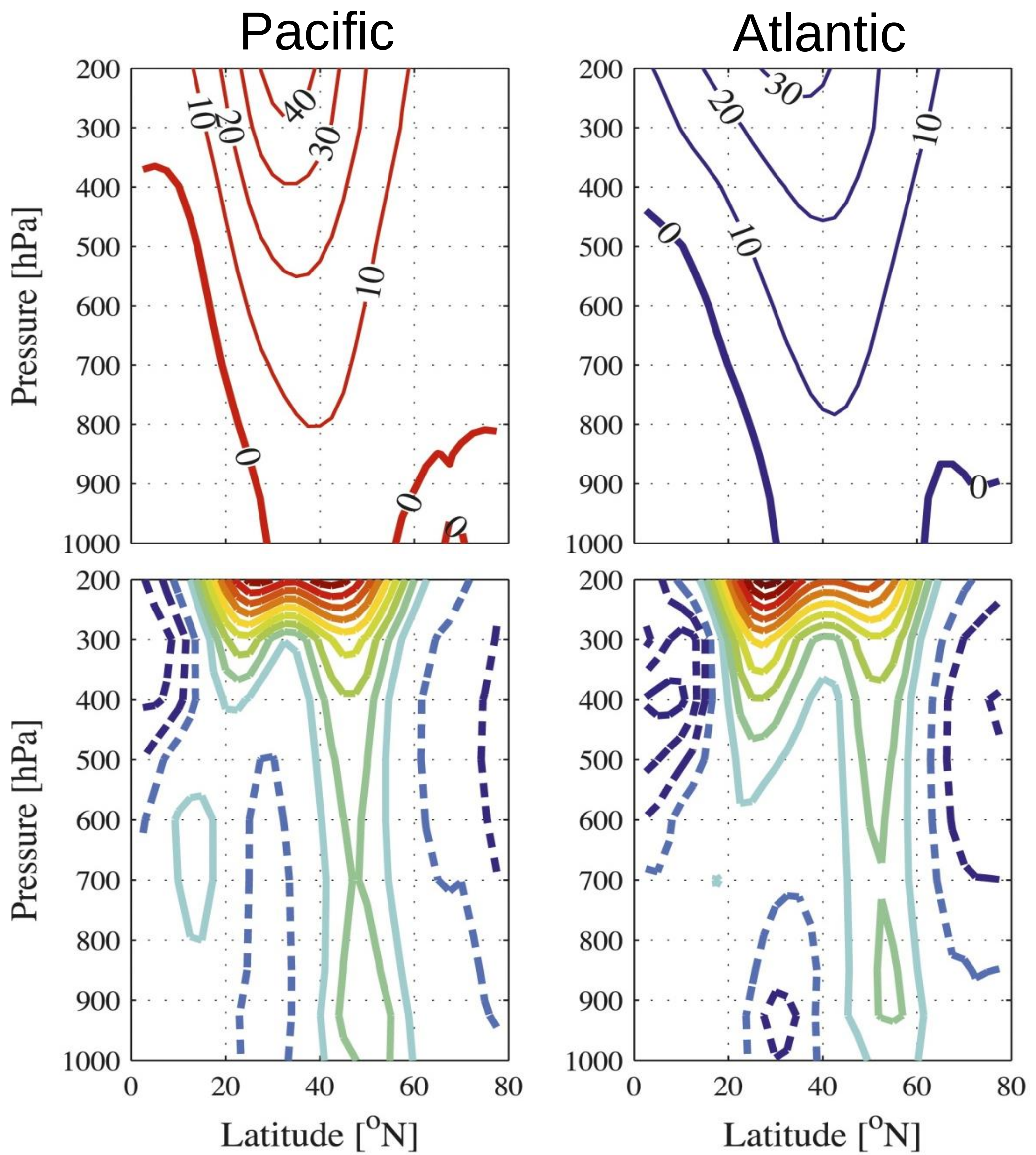

Delcambre et al. (2013)

Clear-air turbulence

Annual-mean vertical wind shear in North Atlantic at 250 hPa (~35,000 feet)

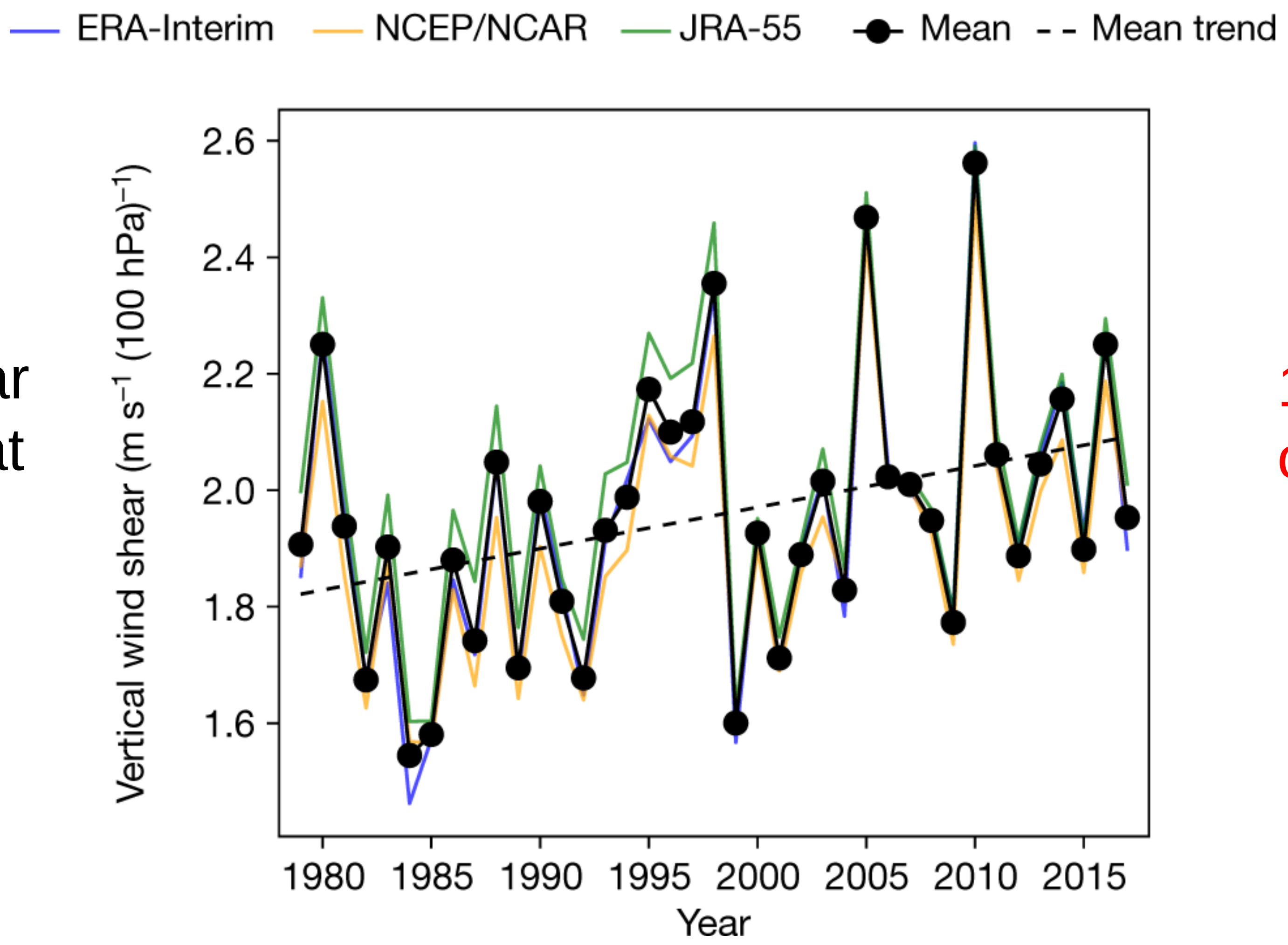

15% increase over 40 years ⇒ more CAT

Lee, Williams, and Frame (2019)

Clear-air turbulence

Winter-mean
CMIP6-mean
vertical wind shear
in Northern Eurasia
at 250 hPa
(~35,000 feet)

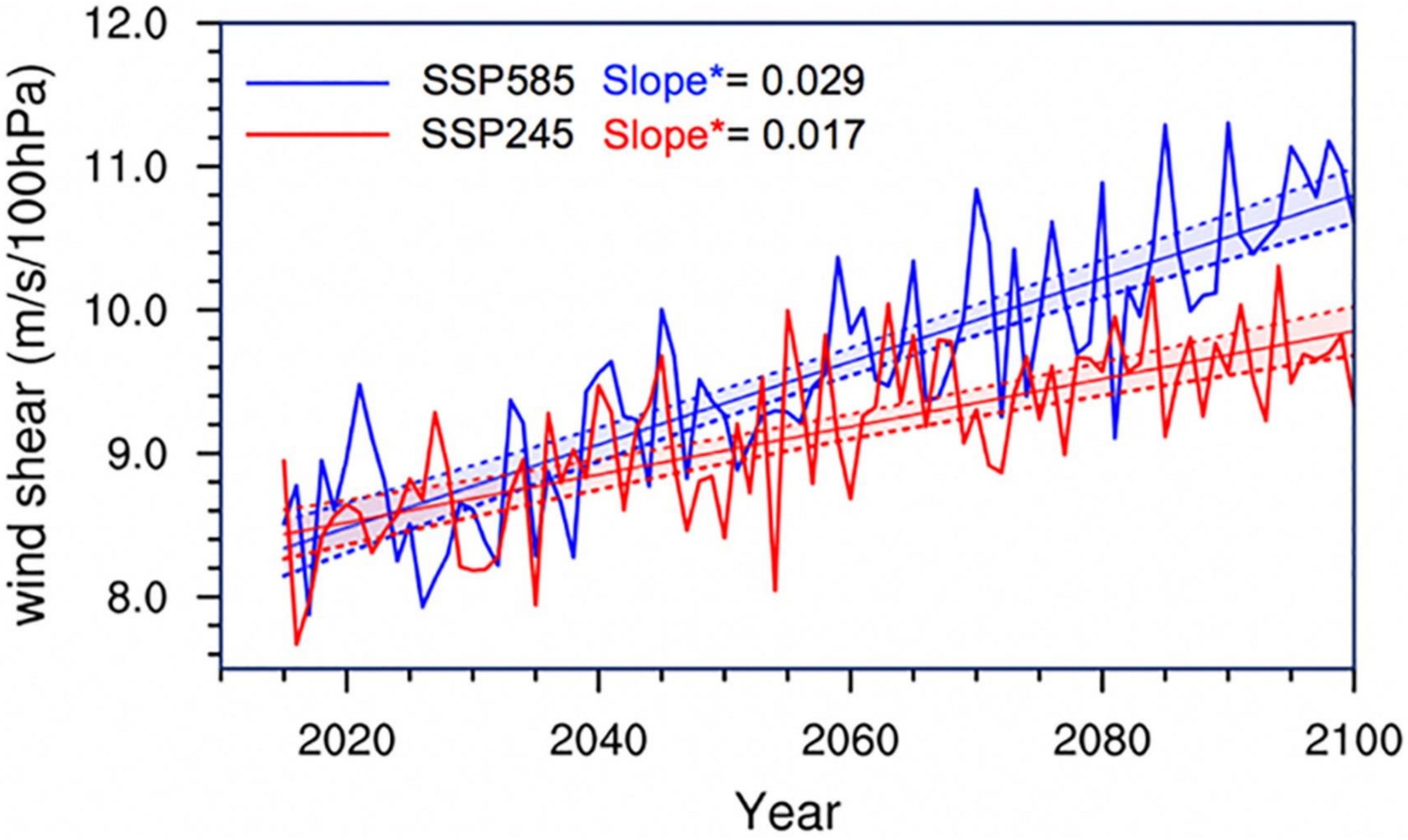

29% increase
over 85 years

17% increase
over 85 years

Lv et al. (2021)

Clear-air turbulence

PRE-INDUSTRIAL

DOUBLED CO_2

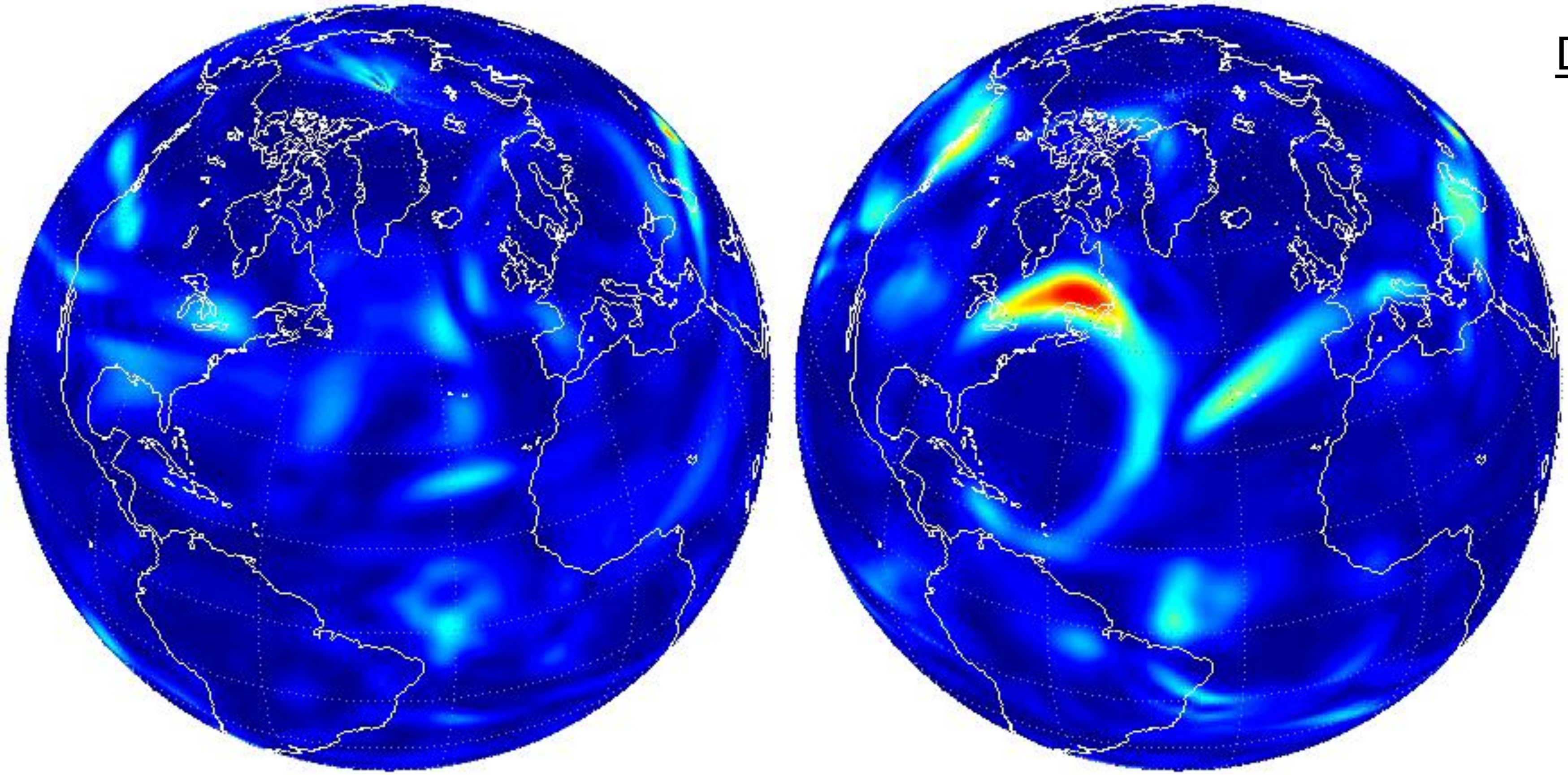

$$TI1 = \sqrt{\left(\frac{\partial u}{\partial z}\right)^2 + \left(\frac{\partial v}{\partial z}\right)^2} \times \sqrt{\left(\frac{\partial u}{\partial x} - \frac{\partial v}{\partial y}\right)^2 + \left(\frac{\partial v}{\partial x} + \frac{\partial u}{\partial y}\right)^2}$$

Williams & Joshi (2013)

Clear-air turbulence

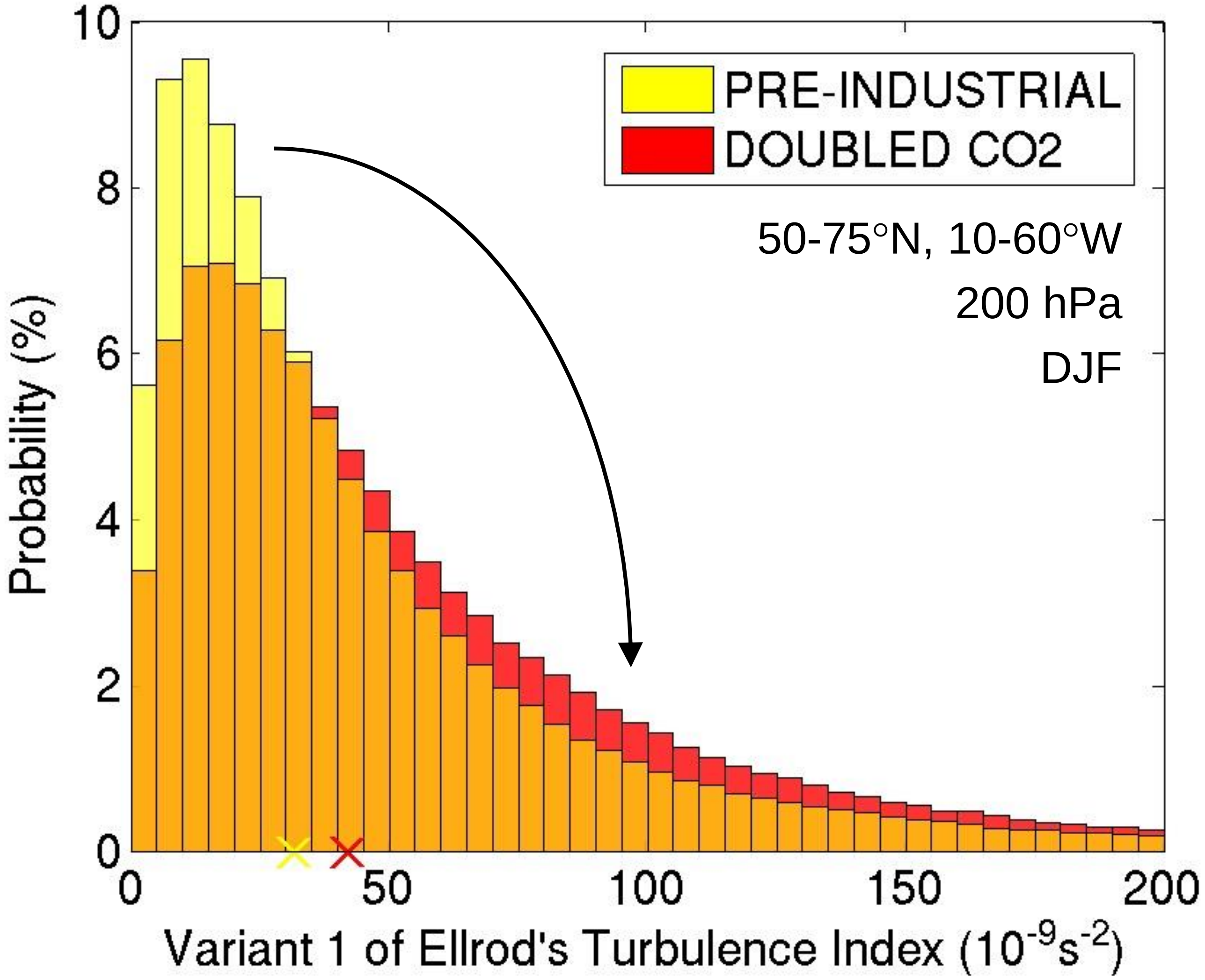

Williams & Joshi (2013)

50-75°N, 10-60°W, 200 hPa, DJF

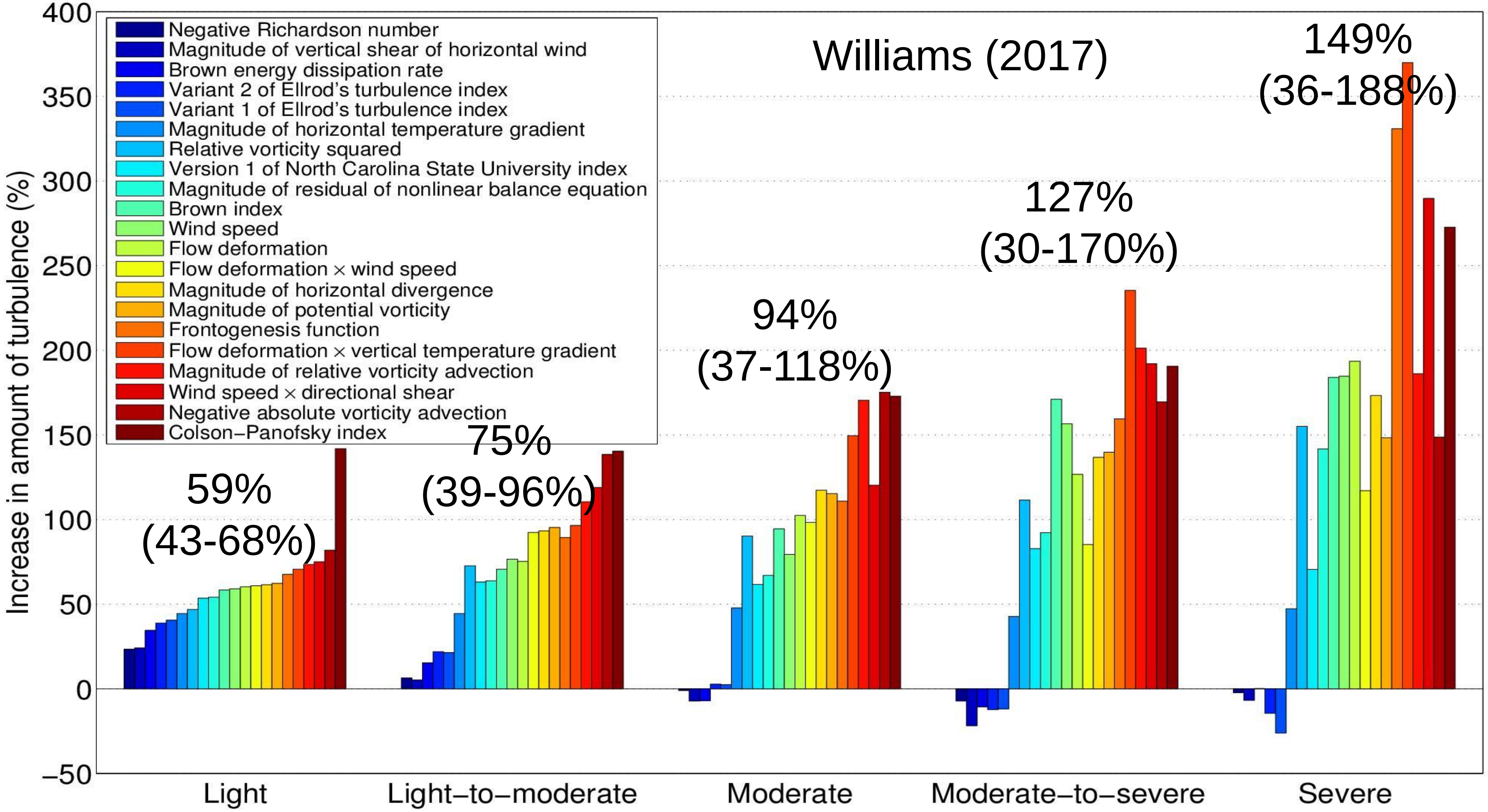

↓

"Slight strain against seat belts; unsecured objects may be displaced slightly; food service may be conducted with little difficulty walking"

↓

"Definite strain against seat belts; unsecured objects are dislodged; food service and walking are difficult"

↓

"Occupants are forced violently against seat belts; unsecured objects are tossed about; food service and walking are impossible"

Clear-air turbulence

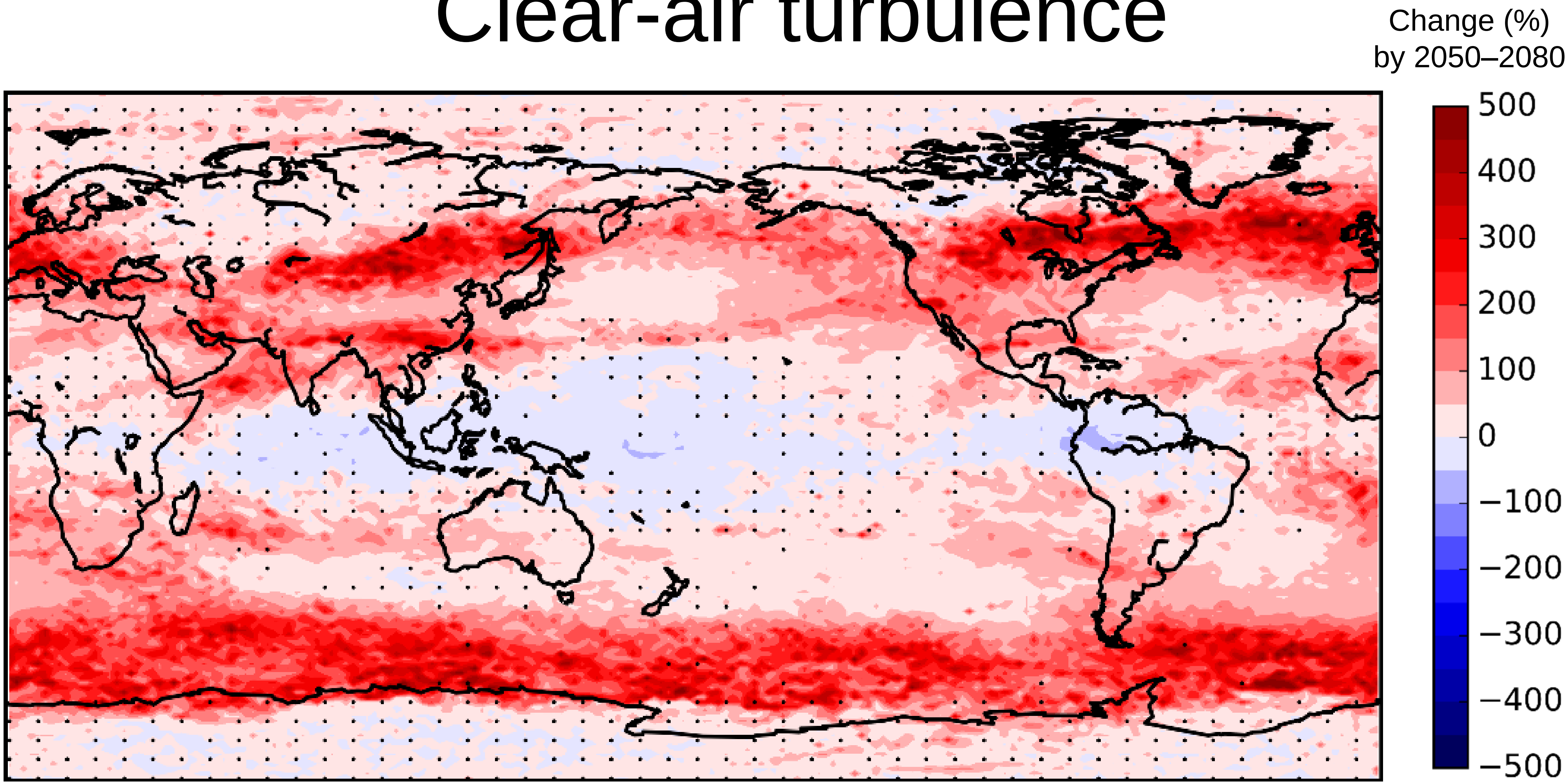

Storer, Williams & Joshi (2017)

Clear-air turbulence

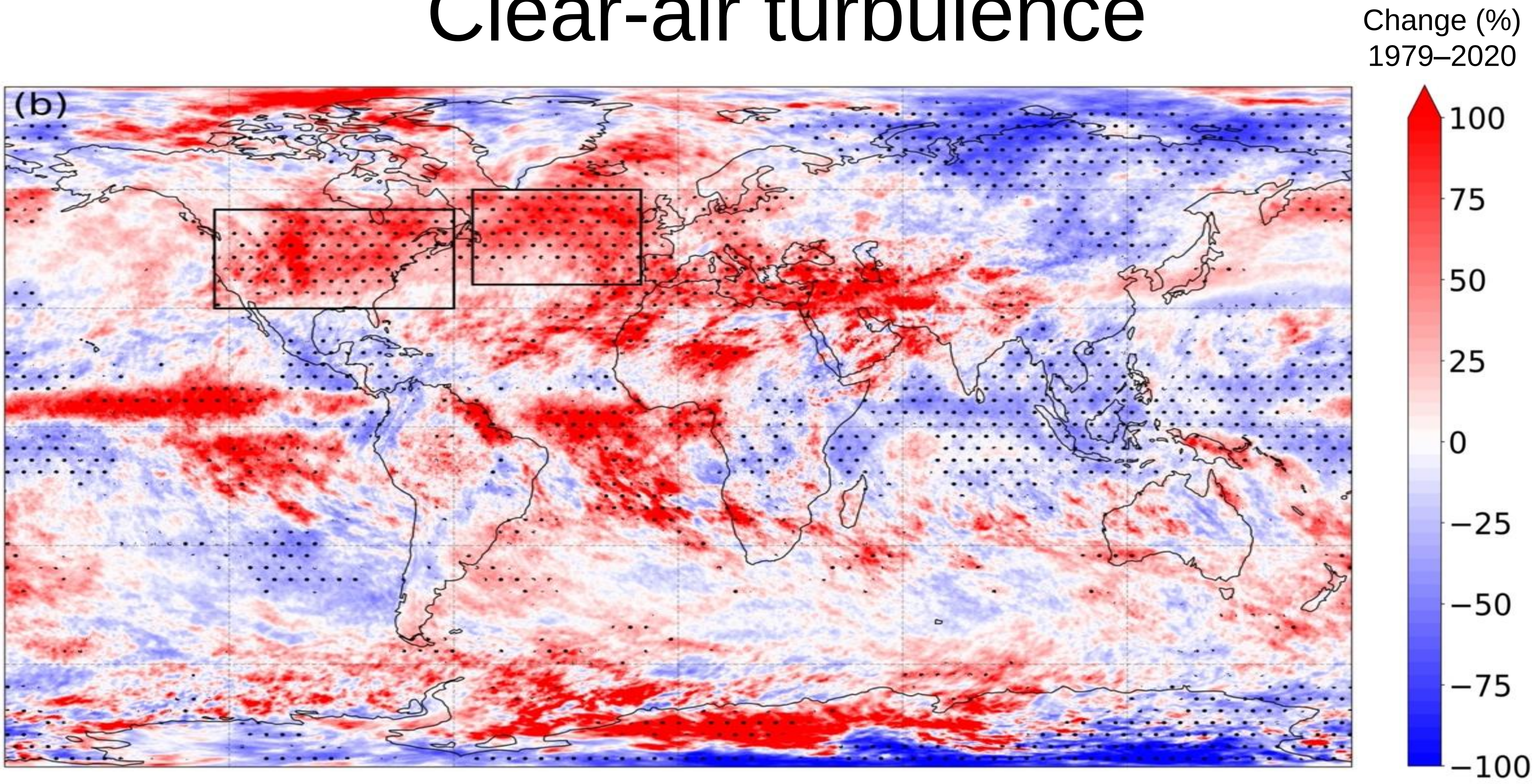

Prosser, Williams, Marlton & Harrison (2023)

Clear-air turbulence

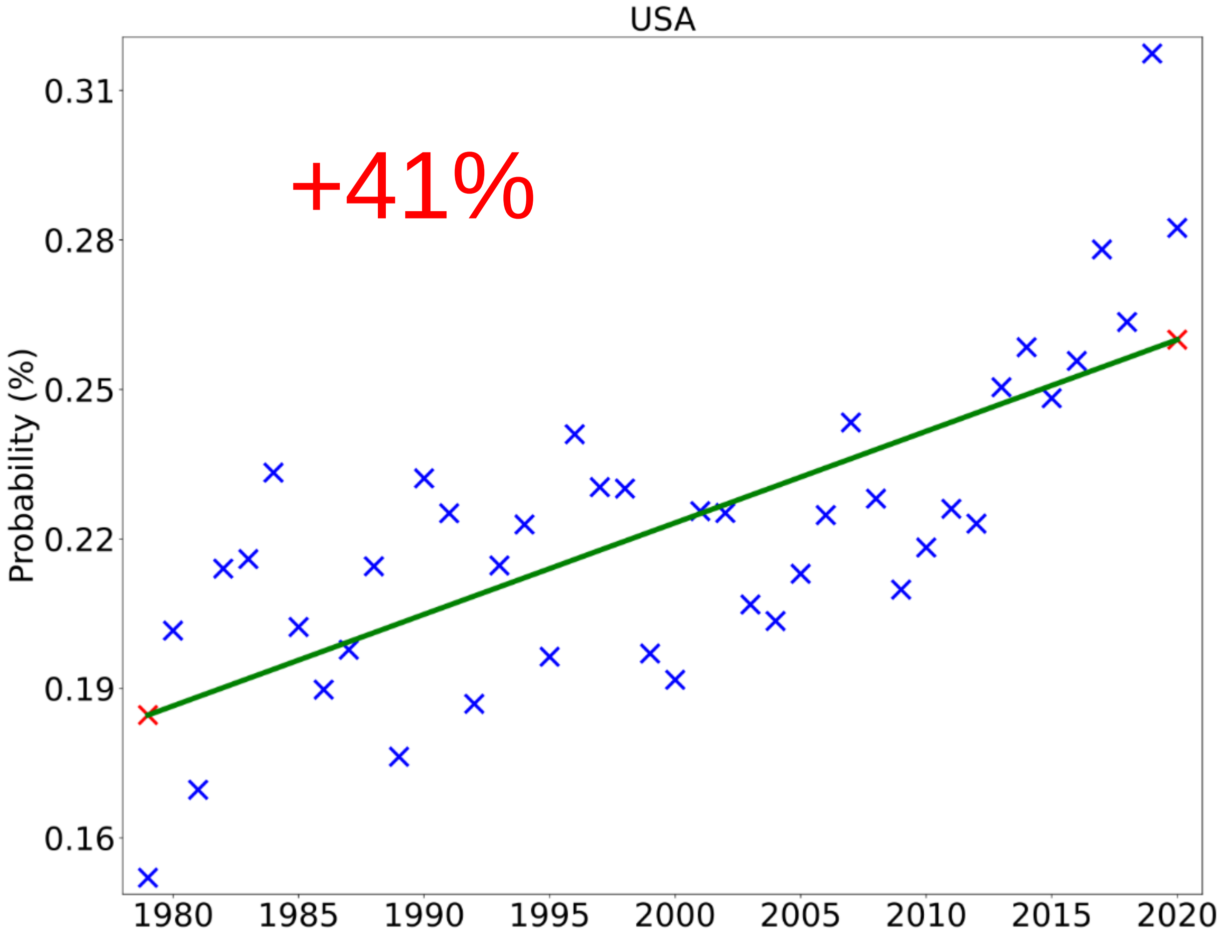

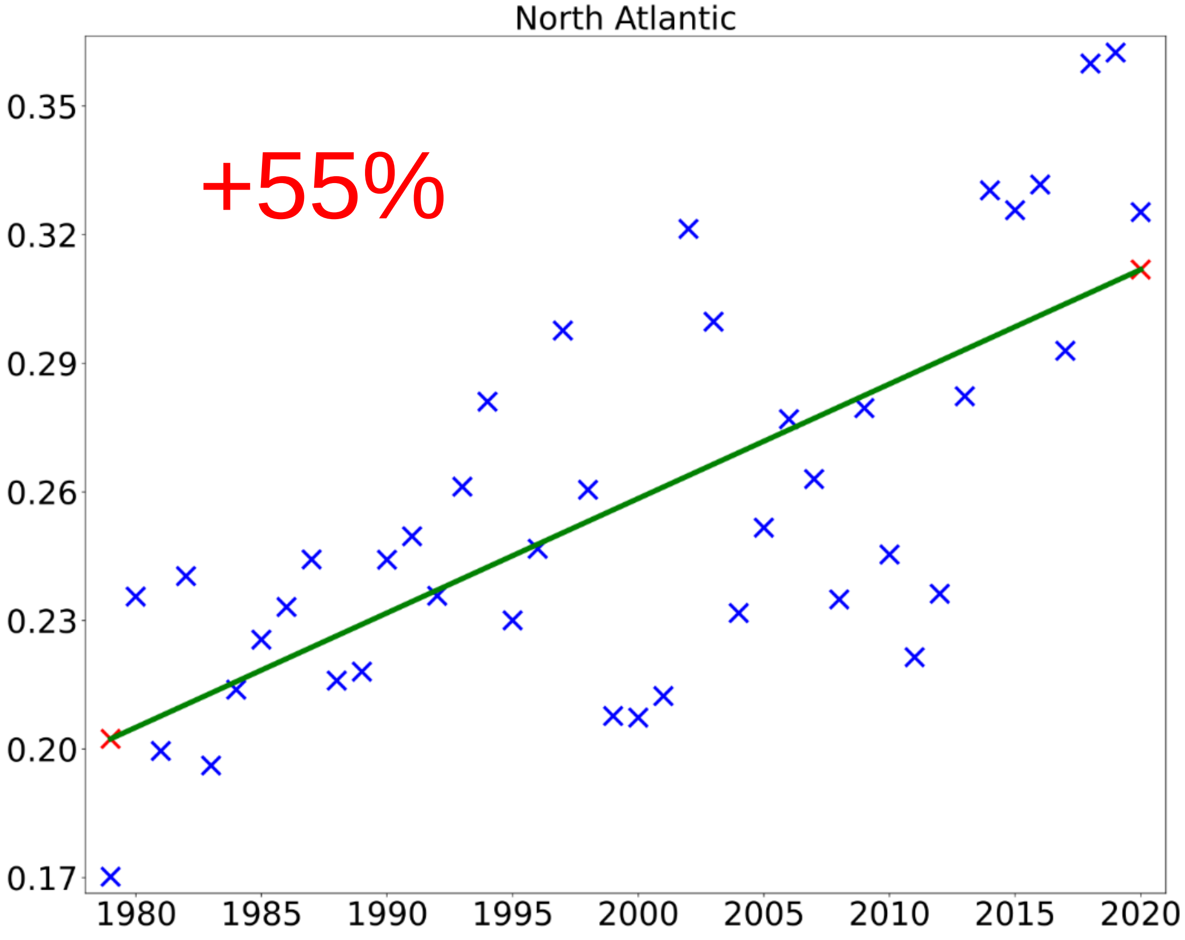

Prosser, Williams, Marlton & Harrison (2023)

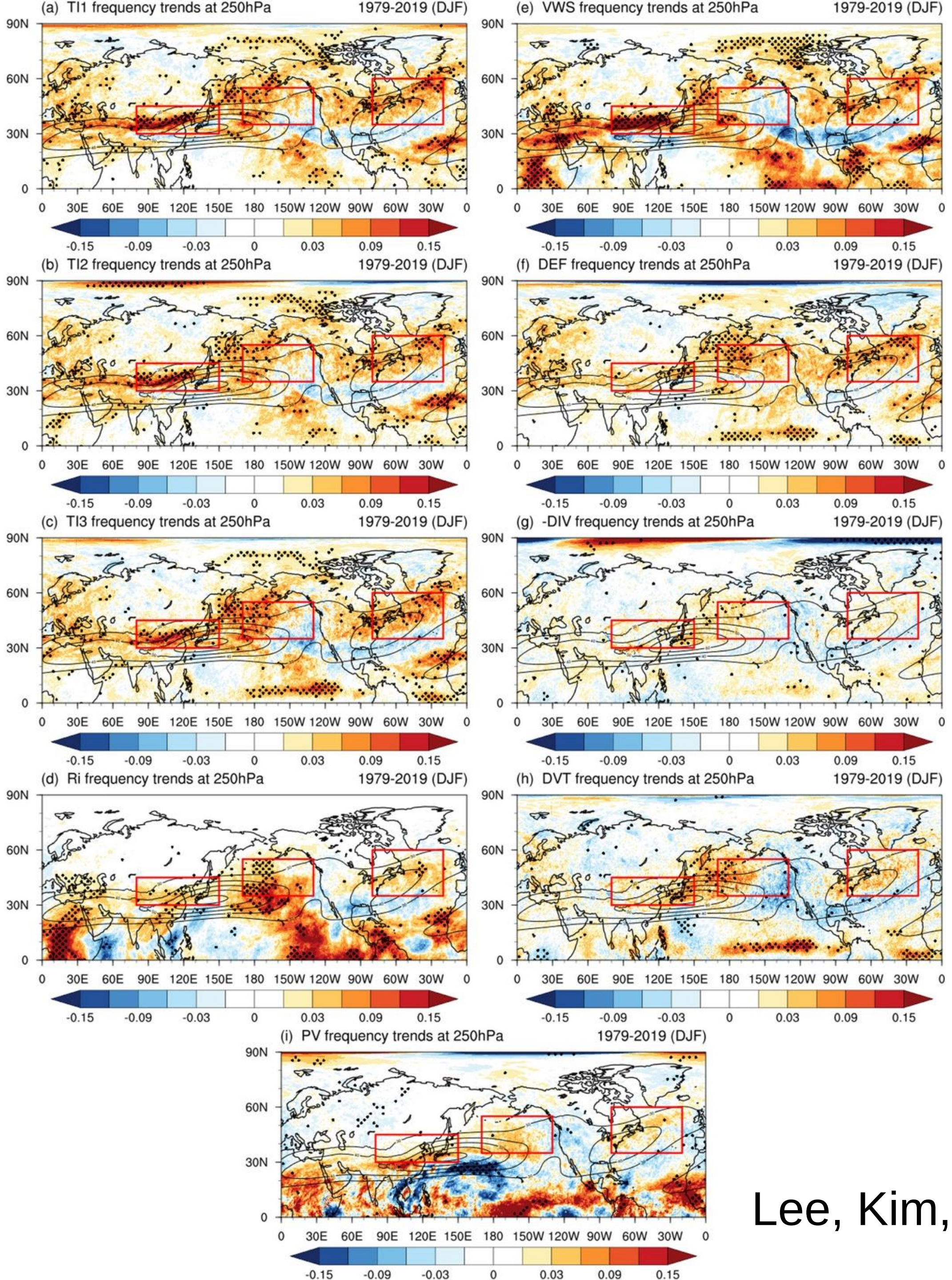

Lee, Kim, Sharman, Kim & Son (2022)

npj | climate and atmospheric science

www.nature.com/npjclimatsci

ARTICLE OPEN

Check for updates

Global response of upper-level aviation turbulence from various sources to climate change

Soo-Hyun Kim[1] ✉, Jung-Hoon Kim[1] ✉, Hye-Yeong Chun[2] and Robert D. Sharman[3]

Atmospheric turbulence at commercial aircraft cruising altitudes is a main threat to aviation safety worldwide. As the air transport industry expands and is continuously growing, investigating global response of aviation turbulence under climate change scenarios is required for preparing optimal and safe flying plans for the future. This study examines future frequencies of moderate-or-greater-intensity turbulence generated from various sources, viz., clear-air turbulence and mountain-wave turbulence that are concentrated in midlatitudes, and near-cloud turbulence that is concentrated in tropics and subtropics, using long-term climate model data of high-emissions scenario and historical condition. Here, we show that turbulence generated from all three sources is intensified with higher occurrences globally in changed climate compared to the historical period. Although previous studies have reported intensification of clear-air turbulence in changing climate, implying bumpier flights in the future, we show that intensification of mountain-wave turbulence and near-cloud turbulence can also be expected with changing climate.

npj Climate and Atmospheric Science (2023)6:92 ; https://doi.org/10.1038/s41612-023-00421-3

Summary

- Measuring turbulence
  - We can directly measure turbulence by bolting accelerometers onto standard radiosondes
  - In over 50 ascents, we have measured accelerations as large as 8g
  - We have used the ~100,000 acceleration measurements to calculate ROC curves and test CAT diagnostics
- Climate change
  - The jet stream is already 15% more sheared than when satellites began observing it
  - There is already 55% more severe CAT over the North Atlantic than in 1979, and 41% more over the USA
  - This effect is projected to double or treble the amount of severe clear-air turbulence in the coming decades